



## RESEARCH ARTICLE

### OSSEO-COMPRESSION ORAL IMPLANTOLOGY, A PARADIGM SHIFT

\*Kianor Shahmohammadi, Gregori M. Kurtzman, Masih Rezaei and Ilia Deylami

31855 Date Palm Dr. Suite 3, #470, Cathedral City, Ca, 92234

#### ARTICLE INFO

##### Article History:

Received 16<sup>th</sup> September, 2017  
Received in revised form  
10<sup>th</sup> October, 2017  
Accepted 27<sup>th</sup> November, 2017  
Published online 27<sup>th</sup> December, 2017

##### Key words:

Fulcrum,  
Lever,  
Polygonal Design,  
One-Piece,  
Impact vs.  
Drill Method Implantology.

#### ABSTRACT

**Purpose:** The aim of this study was to develop a polygonal, solid, and one-piece (1P) dental implant based on the concepts of fulcrum-lever force dissipation and circumferential and apical wedging to maximize initial stability for immediate loading. A threadless implant was designed with a Restorative Attachment and a Bone Engagement Zone as one unit and without any screws.

**Material and Methods:** For this in-vitro study, two random human mandibles were chosen. Impact, drill, and hybrid delivery methods were used to insert 30 prototype dental implants in D1 dense bone zone. Placements were recorded and evaluated with pre- and post-operative CBCT studies and digital photographs. All implants were subjected to Finite Element Analysis and periotest before extraction to evaluate the structural fatigue and stress resistance, initial stability, resistance to micromovement, and amount of autogenous bone graft collected during each delivery method of the new design implant.

**Results:** Regardless of the protocol implemented, initial stability and retention of the polygonal concept exceeded all expectations during the periotest evaluation. Macrogeometries on implant bodies were filled with the bone particle and a significant amount of fine bone was harvested during osteotomy. Although fatigue failure was no longer a concern, FEA demonstrated exceptional structural strength due to strategic design features. The structural integrity of both bone and implants were maintained without any observable microfractures around the osteotomy or delivery sites.

**Conclusion:** With advancements in delivery technologies, impact implantology remains a conservative and an effective alternative delivery method. However, more in-vitro and in-vivo studies are needed. The results demonstrated the 1P fulcrum design provided profound initial stability, the most conservative osteotomy, and controlled ridge expansion. The prototype implants exhibited autogenous bone self-harvesting capabilities in all three delivery methods.

Copyright©2017, Kianor Shahmohammadi et al. This is an open access article distributed under the Creative Commons Attribution License, which permits unrestricted use, distribution, and reproduction in any medium, provided the original work is properly cited.

Citation: Kianor Shahmohammadi, Gregori M. Kurtzman, Masih Rezaei and Ilia Deylami, 2017. "Osseo-compression oral implantology, A paradigm shift", *International Journal of Current Research*, 9, (12), 62403-62422.

## INTRODUCTION

A travelogue through time demonstrates an astonishing journey dental implants have taken to become what they are today. Although it may have been given many looks or delivered differently, operators had only one single goal in mind - that is permanent replacement of lost teeth. From the dawn of implantology, rigid fixation was achieved either by means of wire connection to adjacent teeth, impaction, or drilling into the bone at edentulous areas.<sup>1</sup> It wasn't until the early nineteenth century that J. Maggilio, from France, cast an 18-carat gold tooth-root-shape device, which he utilized and introduced as an immediate implant.<sup>2</sup> The modern and contemporary eras of implantology rolled into history when innovators managed to showcase their brainchildren in display: Strock's screw and nail-like implants in 1939, Dahl's subperiosteal implant in 1940, Lee's endosseous implant with a central post in 1950, Linkow's Vent Plant in 1963 and blade

implant in 1967, Small's transosseous implant in 1975, and Brånemark's most significant two-stage threaded titanium root-form implant in 1977.<sup>2</sup> In 1951, Brånemark had already coined the term osseointegration and developed a two-piece (2P) screw type titanium-threaded implant system. His innovation quickly went viral and gained mass acceptance when he published his pivotal study in 1977.<sup>3</sup> By the 1990's, Brånemark's concept made such an impact in clinical dentistry that mainstream clinicians and public acceptance rose significantly to the extent that it adumbrated all other protocols and systems, specifically one-piece (1P) implants. Improper clinical documentation, inclination towards reports of failed cases, and lack of university based implantology programs accelerated the isolation of the alternative approaches. Failure reports are not scientifically sufficient and conclusive enough to substantiate or refute any techniques or implant systems without proper investigation, hence there are discrepant reports of 1P and 2P success rate.<sup>3-7</sup> However, growth in reception and subsequent demand of dental implant phenomena have put forth considerations for shorter healing periods and better esthetics in last the decade or two.<sup>8,9</sup> Therefore, 1P system is

\*Corresponding author: Kianor Shahmohammadi,  
31855 Date Palm Dr. Suite 3, #470, Cathedral City, Ca, 92234

returning to the spotlight only after many studies<sup>10-25</sup> found 1P and immediate loading (IL) implants superior in terms of implant-bone interface (IBI), surgical protocol, and elimination of potential structural drawbacks of 2P implant in two-stage (2S) protocol. Regardless of the piece-count, initial stability (IS) and long-term success is the driving force behind the dramatic evolution of the implant design. The focus has been to introduce and marry a foreign device into the body as minimally invasive as possible, yet yielding perpetual stability. To achieve such tour de force, multiple components are scrutinized within surgical and biomechanical perspective.<sup>26</sup> Whether one-stage (1S), 2S, or immediate loading (IL), a prosthetic abutment and an anchoring implant body, as the standard pieces, are accompanied by an array of expensive armamentariums and complicated protocols in all 2S-2P implants. In this approach, the implant is inserted into the bone surgically (first stage) followed by a healing screw. After months of prescribed hard tissue healing, a healing abutment is attached (second stage) for soft tissue healing and development of perimucosal seal while the patient awaits another appointment for the final restoration.<sup>27,28</sup> At the second stage, a minute yet redundant uncover surgery may be required to expose implant-abutment interface (IAI), although submerge healing is not a prerequisite of osseointegration.<sup>14</sup> In the case of 1S-2P, the hard and soft tissues are healed at the same time eliminating the second stage surgery and appointment. Finally, IL requires attachment of the prosthetic abutment and final restoration, at the day of implant insertion, leaving healing abutment and screw dismissed.<sup>27</sup> As alluded above, the implant is subjected to rotational load in multiple occasions during the course of the treatment. Considering the very low shear strength of the bone, consecutive tightening and un-tightening of the threaded components of 2P implants may potentially increase the risk of loss of IBI and already achieved IS.<sup>29</sup>

Conversely, both major elements of the 1P implant are manufactured as one unit and practitioners require less than half of the armamentarium. 1P provides unparalleled surgical advantages in terms of surgical simplicity and level of invasion. It is accomplished in only 1S surgical procedure; and, often it is inserted immediately after extraction or flapless with minimal osteotomy, substantially decreasing surgical trauma and post-operative edema, to provide for an uneventful and accelerated healing phase. Furthermore, it is associated with less bone grafting, sinus-lift, and nerve transpositioning.<sup>30</sup> Regardless of the patients' personality type, prolonged treatment period and unnecessary bloodshed are at inconvenience and depict undesirable impressions for already apprehensive ones. The biological width in natural dentition is comprised of a connective tissue attachment (CTA) and a junctional epithelium (JEA), respectively 1.07mm and 0.97mm on average, by which probing depth is determined.<sup>31</sup> Similar to the tooth, biologic tissue encapsulates the implant by generating a band of soft tissue to provide for the integrity of the periodontium and protection from external factors such as mechanical and biological agents.<sup>32</sup> Bone resorption occurs when the epithelium forges a defensive distance as an attempt to isolate the external factors by proceeding beyond them apically.<sup>33</sup> It has been suggested that the location and presence of the microgaps, IAI and abutment-crown interfaces (ACI), are directly related to crestal peri-implant bone loss and stage two uncover surgery of the 2P implants.<sup>34-39</sup> These studies found that exposure of the implant to the oral medium during the uncover surgery allows introduction of bacteria to the barely established biological width eliciting an inflammatory

response and subsequent bone resorption at the crestal region, where the IAI approximates. In 1P implants, the IAI is excluded, the ACI location falls coronal to the biological width, and, thus, the risk of microgap-induced bone resorption is significantly reduced.<sup>37,40</sup> In another study comparing the 1P and 2P implants, the effects of micromovement and size of microgaps at the crestal bone were analyzed and concluded that the more components utilized in an implant system, the higher is the rate of crestal bone loss regardless of the size of the microgap.<sup>41</sup>

Heat generation and dissipation are regarded as major concerns during implant surgery as well as abutment and prosthetic crown preparations.<sup>42,43</sup> Osteotomy preparation is an inevitable direct assault to the labile bone. The resultant surgical trauma can be classified into mechanical and thermal injury from which the bone must recover by utilizing renewed blood supply in order to produce osseointegration at IBI.<sup>44</sup> The amount of prepared bone, depth of osteotomy, and heat generated during drilling is detrimental to the implant success, especially at the crestal regions due to the presence of denser bone and insufficient blood supply.<sup>45-47</sup> Moreover, during prosthetic preparations, frictional heat easily conducts through the metal implant rapidly and jeopardizes osseointegration. Research has defined a thermal threshold of 47°C for 1 minute to avoid subsequent heat-induced cortical bone necrosis and impaired healing. The practitioners are strongly advised to utilize precautionary methods such as frequent coolant irrigation and short working intervals.<sup>48</sup> When compared to 2P implant, 1P requires more abutment preparation by which excessive heat is generated fostering apprehensions amongst clinicians. However, Omer *et al* reported proper water irrigation as beneficial, serving to enhance the cooling capacity of 1P implant significantly and to prevent thermal induced injuries to adjacent hard and soft tissue.<sup>49</sup> In another study on 2P implant, abutment preparation recorded a maximum temperature change of 2°C and 4.7°C, diamond and tungsten bur respectively, using standard turbine and water irrigation system.<sup>50</sup>

“Stress treatment theorem”, according to Misch, “is the key to implant treatment plans.” Unlike the natural dentition, implant lacks the viscoelastic shock absorbing periodontal ligaments while fixated in the bone rigidly; and therefore, the surrounding bone and implant system are at high risks of fatigue and fractures under parafunctional forces. The width, length, and crestal cross-sectional shape of a transosseous structure, implant or tooth, become pertinent in diffusing such offense. The greater the width, the lesser transmitted stress to the bone, the length determines the location, and the cross-sectional shape resists and directs lateral and occlusal loads at the crest.<sup>47</sup> However, in addition to the bone thickness and height limitations as the greatest obstacles to reckon with when choosing the right implant, no implant cross-sectional design comes close to mimic that of a natural tooth. Therefore, from a biomechanical perspective, one of the detrimental aspects in achieving adequate implant-bone approximation, stress distribution, and osseointegration of an implant is its design. Over-all geometry, prosthetic platform and abutment shape, macro- and microgeometries, and material composition define what is referred to as the implant “design”.<sup>51-55</sup>

Improper transition and dissipation of multi-axial functional load and bending moments is menacing to implantology success and marginal bone level preservation. The implant

geometry and its bone-implant contact (BIC) percentage greatly influences load distribution.<sup>8</sup> Exact reproduction of the manner by which natural teeth distribute stress and load to the adjacent bone is improbable by dental implants. However, geometrical similarity between a natural tooth and a tapered implant leads one to speculate that they may abide to similar principles when distributing forces.<sup>56</sup> It has been suggested that tapered (conical) design has proven significantly superior to its counterparts, parallel-walled design, in achieving and maintaining initial stability even in D4 bone zones without any soft or hard tissue complications.<sup>57-64</sup> Although parallel-walled implant scores 20-30% higher in providing surface area for osseointegration and lowering stress in cortical bone in a few studies,<sup>65,66</sup> tapered implant compensates for deficiencies by obtaining much higher values in maximum insertion torque (MIT), maximum removal torque (MRT), and resonance frequency analysis (RFA).<sup>59, 62, 63</sup> The coincidental release of Brånemark's work at the time of technological revolution triggered a movement that led to a multidimensional expansion in implantology in terms of materials and techniques. The material of choice has been titanium since 1940's, when Bothe *et al* observed the very first "bone fusing".<sup>67</sup> Titanium ubiquity is directly related to its chemical and mechanical properties. Anti-corrosive in biological fluid, high strength-to-weight ratio, and machinability are unrivaled qualities that lend titanium "the gold standard" title.<sup>68</sup> Although commercially pure Titanium (cpTi) has proven its clinical success, few alloys have been developed to compensate for its deficiencies. For instance, titanium-aluminum-vanadium alloy (Ti-6Al-4V) has shown to increase cpTi tensile strength at the cost of lower corrosion resistance. As any metal is bound to corrode, Ti-6Al-4V corrosion toxicity was found to produce adverse local and immunological reactions. Yet, the most common commercial dental implants are manufactured from Ti-6Al-4V.<sup>69,70</sup> However, the binary titanium zirconium (TiZr) alloy poses as an integral and improved alternative in that it offers better strength without compromising biocompatibility and osseointegration.<sup>71,72</sup>

In conjunction with material, surface topography or roughness is pivotal complement to osseointegration. Generally, the main idea behind texturing the implant is to maximize surface area and BIC, thus, it is indicated in regions with poor bone quality.<sup>73</sup> So far, three levels have been defined: macro, micro, and nano.<sup>74</sup> Macro-level indeed produces favorable results in respect to initial stability; however, it is associated with ionic leakage and peri-implantitis. Nano-level has been advocated in the past few years as it encourages protein absorption and guides osteoblast adhesion to the titanium surface.<sup>75</sup> Achieving nano-level roughness with current technology deems difficult and expensive. More over, only a few studies have been conducted and many parameters are still unknown in respect to biological quantification and mechanism of action.<sup>74</sup> On the other hand, Micro level yields the maximum bone-implant fixation as well as higher resistance to shear via configuration such as semi-spherical indentations of 1.5um in depth and 4 um in diameter.<sup>76-78</sup> By far, the most common dental implants are the root-form type due to their predictability and relative small size. According to Misch's terminology, the root-form implants are classified based on design into cylinder (press-fit), screw (threaded), or combination design.<sup>27</sup> These models govern the transmission and conversion of occlusal load to the bone and different types of forces: compressive, shear, and tensile. Therefore, strategic engineering designs become more important than ever to counter and prevent the destructive

shear and tensile forces.<sup>29</sup> While the press-fit type benefits from macro- and microgeometries (e.g., surface topography, semi-spherical indentations) to obtain microscopic bond to the bone, screw type affixation is by means of microscopic elements of threads on the body of an implant.<sup>27</sup> The best-known macro- and microgeometry designs and textures for osseointegration play major role in maintaining structural integrity of bone and implant as well as enhancing the rate and quality of bone-implant fixation. It is pertinent to mention that simply designing a perfect implant does not diminish the need to examine the cause(s) of implant failure, although science has yet to designate an exact reason for rejection.<sup>79</sup> However, consensus is when establishment and/or maintenance of osseointegration is jeopardized or impaired, at early stages of bone healing, implant mobility is rendered as the epitome of unsuccessful implant surgery.<sup>81-83</sup> To date, geometrical studies on implant design have not investigated alternative shapes other than circular or oval in cross section of bone engagement. The aim of this in-vitro study was to develop a 1P, threadless, tapered, and hexagonal (in cross-section) implant design for immediate loading. It utilizes the concepts of fulcrum-lever force dissipation and wedging circumferentially and apically for initial stability while enhancing the clinical and functional aspects. It was assumed that the results of the present study would make it possible to explore alternative possibilities other than common implant devices, delivery methods, and protocols in implantology.

## METHODOLOGY, RESULTS AND MATERIALS

### Pilot Study

Before commencement of the actual experiment, a pilot study was performed on two swine and one human mandibles using pre-prototype implant designs to determine the following:

- 1) Functionality, feasibility, and possible modifications of the pre-prototype implant
- 2) Estimation of force of impact for D1-D5 bone
- 3) Identifying the most appropriate surgical protocol

Subsequent to this knowledge, proper modifications were implemented to the main experiment.

### Pilot Study Material

#### 1) 6 Pre-Prototype Implants (PPI)

All the PPIs (Photo 1) were solid and 1P with chisel-like apical portion and hexagonal in cross-section at the bone engagement zone. 4 PPIs were parallel-walled from end-to-end, while 2 were designed with slight tapering from the bone engagement to coronal-end portion to investigate potential capabilities for multi-unit restorations. They all measured at 4.5x3x22 mm at the widest portion and milled from Titanium Grade IV.

#### 2) Piezotome 2

ACTEON® piezoelectric ultrasonic generator at 28-36 mHz was used utilizing following tips: 1) Ninja tip 2) CS1-5

#### 3) Implant Surgical Kit

#### 4) Dental Mallet

#### 5) Industrial Grade Electric Hammer

#### 6) 2 Swine Mandibles (Sierra, Whittier, Ca)

1 Human Mandible (Skulls Unlimited International Inc., Oklahoma City, OK)

- 7) Conventional high-speed handpiece  
8) Sectioning bur 703FG

### Pilot Study Methodology

Three experiments were designed for this pilot study. The first experiment (SM1) included preparation of six osteotomies with Piezotome 2 and placement of six pre-prototype implants (PPIs) in a swine mandible. The second experiment (SM2) included preparation of six osteotomies with implant surgical kit and placement of six PPIs in the other swine mandible. The final experiment (HM) included preparation of six osteotomies, three with a surgical kit and three with a Piezotome 2, for placement of six PPIs in a HM specimen. In each experiment, three PPIs were tapped into final length by an industrial electric hammer, while a dental mallet was utilized to tap the other three to final length. The two SMs were used first to evaluate protocols and instrumentations on ex-vivo fresh bone. The HM specimen aided in evaluation of osteotomy preparation protocol and PPIs feasibility for the main study. The HM specimen included a combination of edentulous and immediate sites. Complete surgical protocols were carried in each experiment while the PPIs were re-used from one specimen to another. Flow chart 1 illustrates the pilot study design.

#### Swine Mandible #1 (SM1)

A mucoperiosteal flap surgery was performed to expose the bone in D1 bone zone using a surgical #15 scalpel blade and #9 periosteal elevator. Following manufacturers operating instructions, Piezotome 2 Ninja tip was utilized to create the pilot holes and followed by CS1-5 tips for modification and preparation of the osteotomies at 7mm length. Then, the PPIs were placed into the osteotomies and tapped to 10 mm final length. All prototypes were extracted following conventional extraction techniques similar to that used for human patients after thorough evaluation.

#### Swine Mandible #2 (SM2)

A mucoperiosteal flap surgery was performed to expose the bone in D1 bone zone using a surgical #15 scalpel blade and #9 periosteal elevator. A703FG bur at 2000rpm was used to penetrate crestal bone vertically for 7mm pilot holes. Six PPIs were placed into the osteotomies and tapped to 10 mm final length (Photo 2). All prototypes were extracted following conventional extraction techniques similar to that used for human patients after thorough evaluation.

#### Human Mandible (HM)

A 2.4mm diameter tapered-tip pilot drill was used to prepare three 7mm vertical initial osteotomies on the right side. This step was followed by osseous expansion with a 5.0x8mm and 4.25x10mm conical drills with corresponding stoppers. Three PPIs were driven to 7mm length of osseous engagement zone using a surgical handpiece at 45 N/cm. Three osteotomies were produced using Piezotome 2 following the same protocol mentioned in SM1 experiment on the left side. The PPIs were tapped to 10mm final length (Photo 3) and extracted following conventional extraction techniques similar to that used for human patients after thorough evaluation. Post-op evaluations were conducted with CBTC and photographs.

### Pilot Study Results

#### Pre-Prototype Investigation

Upon complete insertion, it was determined that rotating the PPI's within the osteotomies was impossible under high torque. An Industrial grade plier had to be used for extraction due to PPI's rigid fixation. It was evident that considerable amount of fine bone was collected within macrogeometries of bone engagement portion (Photo 4). Structurally, all PPI's and mandible specimens withstood the force of impaction and extraction firmly without any signs of fatigue or microfracture around the osteotomies.

#### Protocols and Delivery Methods Investigation

With concentration on protocol efficiency and practicality, the objectives were to perform a mucoperiosteal flap surgery, to evaluate the use of Piezotome for implant site preparations, and to tap PPIs D1 bone. In SM1 experiment, the process of osteotomy preparation in D1 bone was surprisingly not as efficient as expected. To produce desired bone modifications, Piezotome 2 required switching in-between a few different tips that had to be fitted and tightened properly. Additionally, it deemed physically demanding to penetrate 7mm into D1 bone. The over all performance of Piezotome was time consuming, although it performed viably in bone density of D2 to D4. In SM2, implant surgical kit facilitated the process. Although it required switching drill bits and fewer pieces when compared to Piezotome 2, less time was consumed for osteotomy preparation. In HM experiment, utilizing implant surgical kit and associated protocol was determined superior than Piezotome 2 in osteotomy preparation in D1 bone once more. For pilot holes, it was assumed more efficient and facilitating to use a cylindrical surgical bur with dimensions slightly smaller than PPI's. The dental mallet performance was less vigorous and efficient than the industrial electric hammer, as expected, in all experiments.

#### Pilot Study Conclusion

Pre-prototype implants confirmed assumptions regarding the PPIs feasibility to achieve profound initial stability. Although 7mm osteotomy length resulted in desired initial stability, it was determined to prepare them at 8mm so that less tapping would be required to fully seat the implants in the main study.

#### The following PPIs design modifications were decided for the main experiment:

- 1) Changing from parallel-walled to tapered root form design to improve implant-bone fixation even further.
- 2) Include biological width of 2-3mm at the crestal bone engagement zone with a platform switch.
- 3) Design a solid 3x2x8mm hex abutment portion with 1mm margin as platform switch.
- 4) Design a sleeve/margin system to slide over the hex abutment portion for pick-up impression and prosthetic fabrication.
- 5) Design a matching carrier for handpiece and torque wrench to engage the hex abutment portion for insertion torque, harvesting autogenous bone, and assuring proper orientation during placement.
- 6) Increasing proposed osteotomy length from 7mm to 8mm

Titanium Grade IV was selected as the material of choice due to its superb mechanical and chemical properties. Regarding the protocol and delivery methods, in terms serving the study objectives and purpose, there was a significant performance difference between Piezotome 2 and implant surgical kit protocol. Therefore, it was decided to eliminate the use of Piezotome 2 and utilize surgical kit protocol and tapping method for the main experiment. Further investigations with Piezotome 2 need additional studies in the future.

## Main Study

### Main Study Methodology

In this study, the term “hybrid” refers to a combination of impact and drill methods. Also, “regular and irregular hex” refer to the cross-sectional shape of the implant prototypes. Regular hex is a symmetrical hexagon geometrically; while in the later, only two parallel planes of hexagon are equally and slightly longer than the other four planes in cross-section. Two human mandible specimens (Photo 5) were chosen to perform All-On-6 substructures. The condition of each specimen was as following: one fully edentulous (FEM) and one with extracted sites (EM). Impact, drill, and hybrid delivery methods were used to insert 30 prototype dental implants in D1 bone zones. Initial anatomical landmarks were examined via pre-operative CBCT (CBCTs 1 and 2). Surgical kit drills were utilized to prepare osteotomies with respect to anatomical structures such as mental and inferior alveolar nerves. All the prototype implants were fabricated from Titanium Grade IV according to specific chemical compositions (Table 1) and mechanical properties (Table 2). Flow chart 2 illustrates the main study design. A total of 30 prototype dental implants were divided into 2 groups. In group 1, 15 Regular Hex Polygon Prototypes (RHPP) (Photo 6) and the FEM specimen were dedicated to the drill and hybrid methods. It was decided to utilize two delivery methods for placement of RHPPs for further analysis. In group 2, 15 Irregular Hex Polygon Prototypes (IHPP) (Photo 7) and the EM specimen were dedicated to the impact method only. Although all implants were 16mm in total length with a 10mm osseous engagement zone, RHPPs greatest width marked at 4.39mm and IHPPs greatest width were 4.20mm. Figures 1 and 2 demonstrate dimensional specifications for both prototypes.

### Group 1: RHPP – Hybrid method

8mm vertical osteotomy preparations were made for placement of seven RHPPs. A precision drill was used to penetrate crestal bone for guiding holes. Then, a 2.4mm diameter tapered-tip pilot drill was used to prepare 8mm vertical initial osteotomies. This step was followed by osseous expansion with a 3.8x8mm and 4.25x8mm conical drills to a final depth of 8mm. RHPPs were initially driven to 8mm length of osseous engagement zone using a surgical handpiece at 45 N/cm (Photo 8). Then, they were impacted into an additional 2mm with a dental mallet.

### Group 1: RHPP – Drill method

10mm vertical osteotomy preparations were made for placement of eight RHPPs. A precision drill was used to penetrate crestal bone for guiding holes. Then, a 2.4mm diameter tapered-tip pilot drill was used to prepare 10mm vertical initial osteotomies. This step was followed by osseous

expansion with 3.8x10mm and 4.25x10mm conical drills to a final depth of 10mm. RHPPs were driven to 8mm length of osseous engagement zone using a surgical handpiece at 45 N/cm. Then, they were tightened further with a ratchet to a final depth of 10mm.

### Group 2: IHPP – Impaction method

A703FG bur and a surgical stent were used to penetrate crestal bone vertically for 5mm pilot holes. Then, the prototypes were tapped to the final length of 10mm using an industrial-grade electric hammer guided by a carrier. All placements were studied with post-operative CBCT studies (CBCTs 3 and 4) and digital photographs (Photo 9). Additionally, Periotest was conducted to measure initial instability and resistance to micromovement of all the implants before extraction (Photo 10) and evaluating the amount of autogenous bone graft collected during each delivery method.

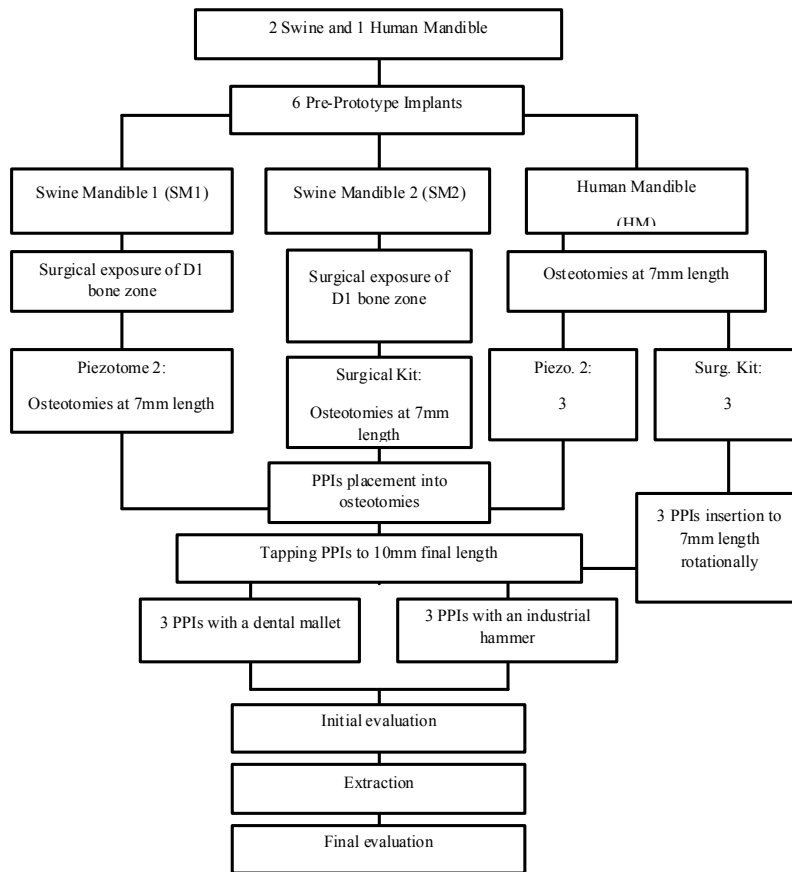
## Main Study Materials

### Topography and Design

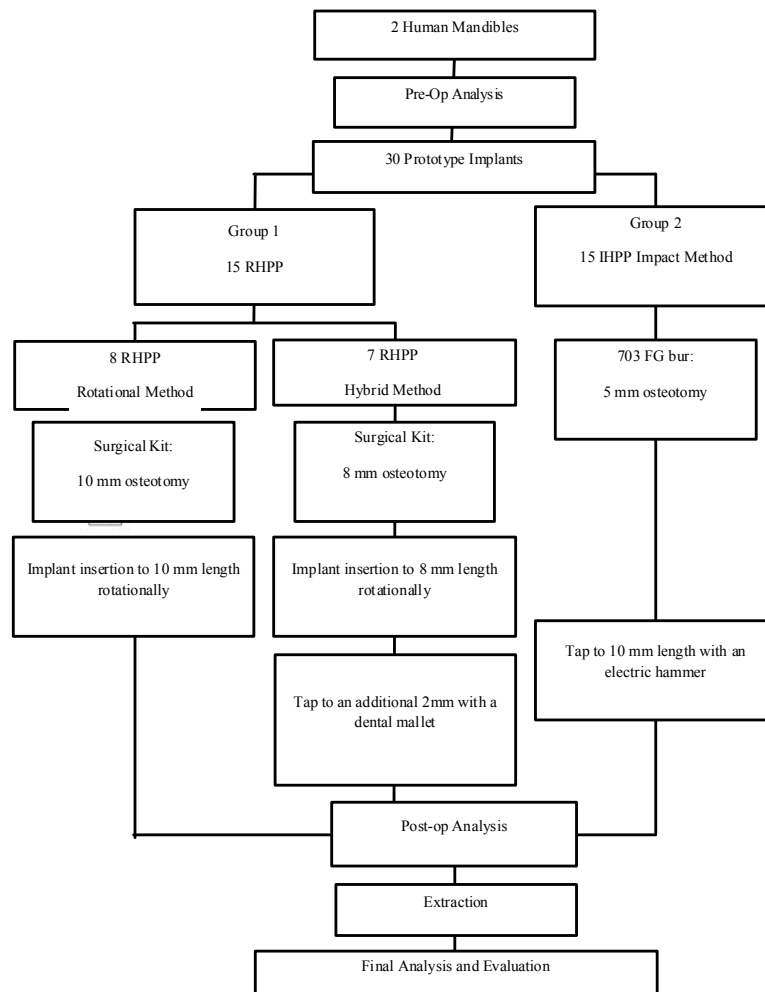
All prototypes were a 16mm long, one of a solid hexagonal structure in cross section of the Bone Engagement Zone (BEZ). A gradual taper mimics the shape of a root of the natural dentition from the Crestal Zone (CZ) to the apical end portion of the implant, such that, the implant device is thicker and wider at the BEZ than at the apical end portion (Figures 3). By design, this prototype is divided into multiple zones each serving a/or multiple purpose(s). The 6mm Restorative Zone (RZ) is comprised of 3mm Attachment Zone (AZ) and 3mm Prosthetic Margin Zone (PMZ). Whereas, 3° taper is evident from the top of the RZ to the platform switch in IHPPs (Figure 2), RHPPs experience such taper only at the PMZ and its AZ remains parallel to the long axis of the device (Figure 1). Geometrically, the RZ is designed to accommodate for multi-unit restorations and delivery systems to engage an external hex at the most coronal 3mm of the prototype. The PMZ in collaboration with the initial 2mm of the Implant Body Zone (IBZ) provide the 5mm Machines Surface Zone (MSZ), which aids to prevent plaque accumulation. The 2mm Crestal Zone (CZ) represents the transition zone from the PMZ to IBZ at the crest of the ridge. A total of 36 semi-spherical indentations, which acted as autogenous bone graft reservoirs in this study, are engraved onto the 6mm Harvesting Zone (HZ) linearly, 6 on each plane and 1 mm deep at the most concave point. All the planes and beveled corners converge harmoniously into a chisel-like apical end portion to form the 2mm Fulcrum Zone (FZ). The 10mm BEZ is referred to the IBZ and FZ collectively (Figure 3).

### Finite Element Analysis

The Bone Engagement (BEZ) and Restorative Zone (RZ) of the RHPP and IHPP were subjected to a series of comparative behavior of fatigue failure. Four types of spherical titanium alloy coping (Ti-6Al-4V Gr. 5) was attached to each RZ to ensure the uniform transfer of applied load while stimulating prosthetic crowns of various lengths. Additionally, load was applied at 30° angled to better approximate standard masticatory force vector in the worst-case scenario. Four IHPPs and one RHPP implants were embedded onto separate bases.



Flow Chart 1.



Flow Chart 2.

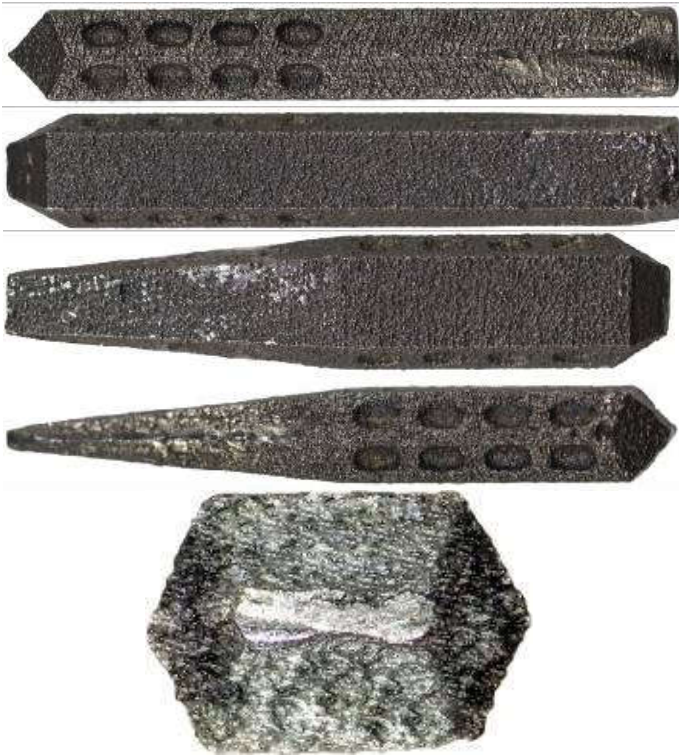


Figure 1. Straight and Tapering Pre-Prototype Implants

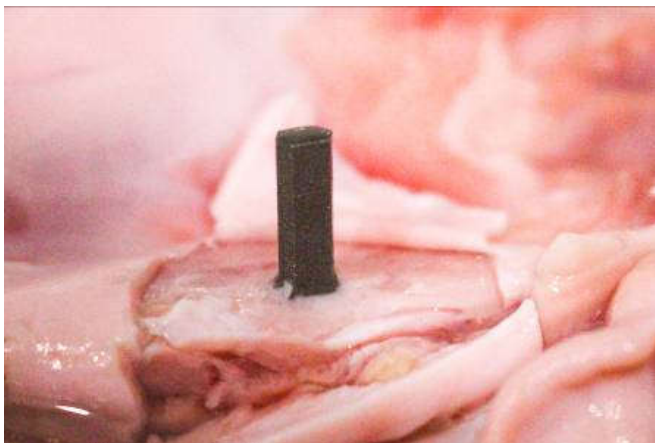


Figure 2. Fully seated PPI in SM 2



Figure 3. Fully seated PPIs in HM



Figure 4. Bone particles with in PPI reservoirs



Figure 5. Mandible Specimens: IHPP group (Left) and RHPP group (Right) Pre-Op.

The objective was to evaluate the differences in the FEA and the maximum load that the best configuration test could tolerate during a fatigue test in multiple scenarios. Table 3 illustrates the testing conditions for each implant in details. The Mathematical calculation model of the implants was obtained by means of tetrahedral solid elements. The structural analysis was conducted in a linear elastic field. Therefore, a linear increase in maximum stress in bone was expected. The interface between the titanium alloy coping and the RZ was considered continuous.

**Load and Constrains Application Method**

The structural analysis is conducted by applying a unit load at an intensity of 1N in accordance with the standard requirements. The linear elastic analysis allows applying the principle of superposition for determining the limit load of static resistance and fatigue resistance. In case of implants that do not have pre-angled components, the UNI EN ISO 14801:2017 standard requires that the load applied has a straight line of action, forming an angle of 30° with the axis of the implant. The fixture must be embedded onto a base so that the nominal bone level is distant 3 mm from the connecting section to stimulate bone resorption. The test scheme indicated by the standard is reported below.

**Method adopted to test the fatigue resistance: General references**

Because of the geometric configuration of the implant, the constraint conditions and load applied, the stress present in the implant itself is a triaxial type of stress. Therefore, all the possible stress components are present. With reference to the reference system chosen, the following stress components are present:

- $\sigma_x, \sigma_y, \sigma_z$ : Normal stress components along the x, y, z axes.
- $\tau_{xy}, \tau_{xz}, \tau_{yz}$ : Tangential components of idle stresses on the xy, xz, yz planes

**With reference to the principal directions, the following stresses are present:**

$\sigma_1, \sigma_2, \sigma_3$ : Stress components along the principle directions  
 In order to calculate the fatigue resistance, it is necessary to introduce two values too:

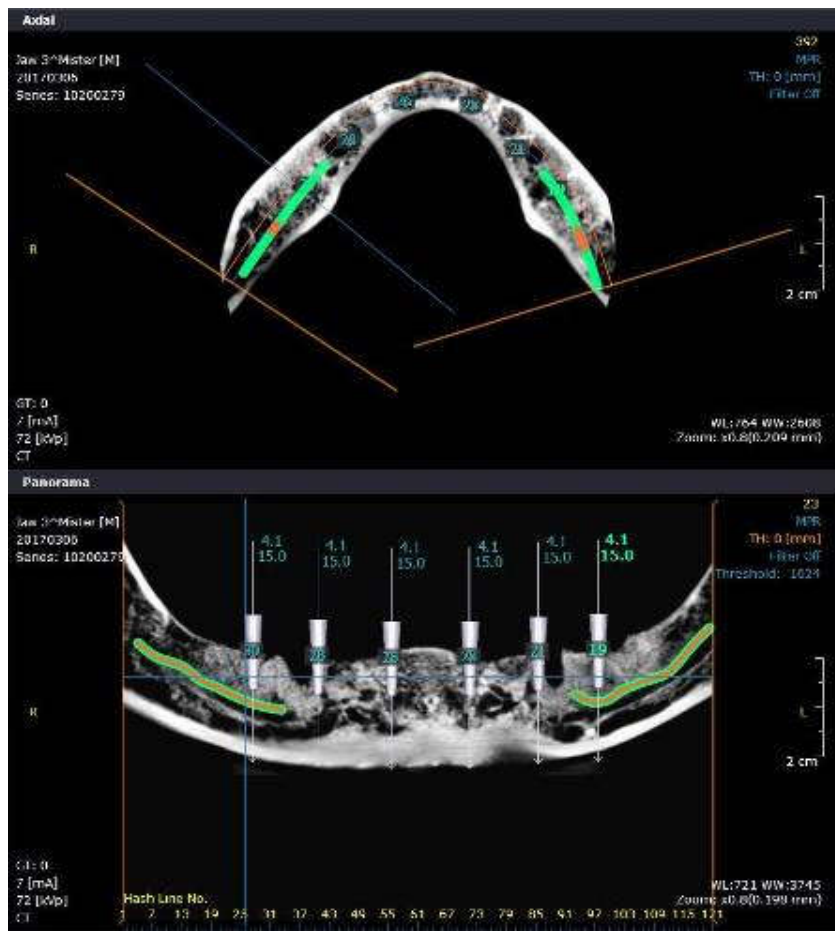


Figure 6.

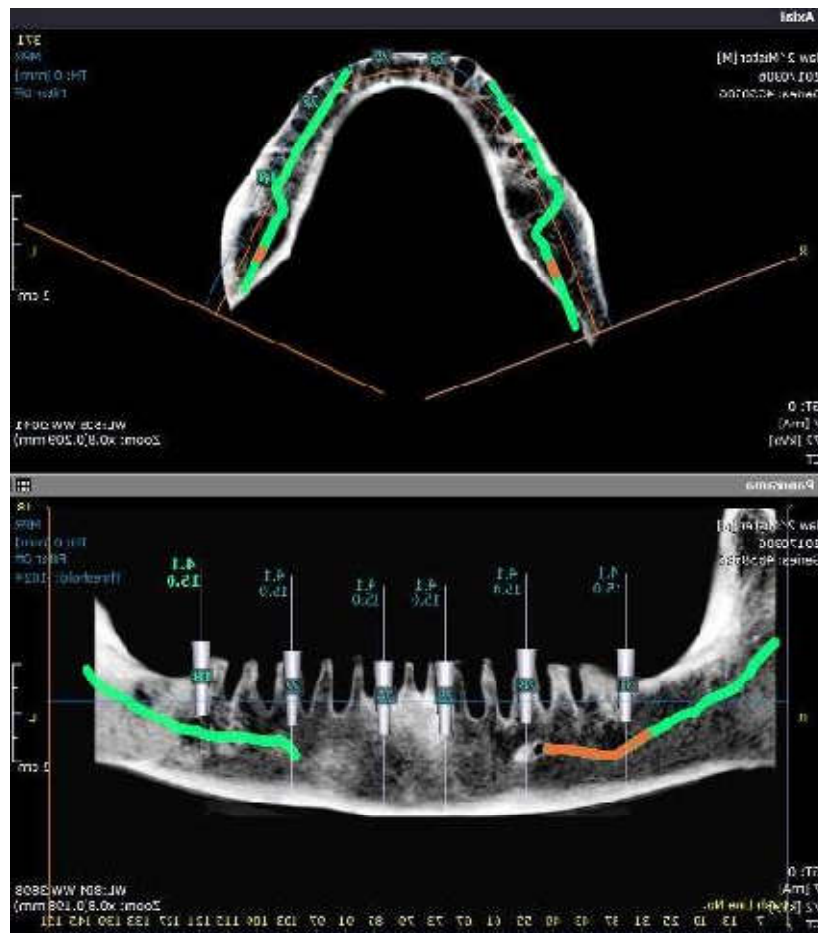


Figure 7.

**Table 1. Chemical Composition of Titanium Grade IV**

Chemical Composition	Maximum Allowed Values (%)	Tolerance
Nitrogen	0.05	+/- 0.02
Carbon	0.08	+/- 0.02
Hydrogen	0.015	+/- 0.002
Iron	0.50	+/- 0.10 (%<0.25) +/- 0.15 (%>0.25)
Oxygen	0.40	+/- 0.02 (%<0.20) +/- 0.03 (%>0.20)
Titanium	Remainder	-

**Table 2. Mechanical Properties of Titanium Grade IV**

Mechanical Properties	Minimum allowed values (%)
Tensile strength	680 MPa (N/mm <sup>2</sup> )
Yield strength (0.2%)	520 MPa (N/mm <sup>2</sup> )
Elongation at yield	15%
Necking	25%

**Figure 12. RHPP Implant Insertion Assembly**

- The fatigue test aims at determining the value of the external load applied to the system which ensures a duration equal to that provided for by the UNI EN ISO 14801 standard.
- This rule identifies two different duration values to be adopted in relation to the frequency of the load application. In fact, with a frequency of  $f \leq 2\text{Hz}$  the requested duration is equal to  $2 \cdot 10^6$  cycles.
- With a frequency of  $f > 2\text{Hz}$  the requested duration is equal to five  $\cdot 10^6$  cycles.
- The fatigue resistance is calculated by assuming a test frequency of  $f > 2\text{Hz}$ .
- Consequently, the maximum applicable load will be calculated for having an implant duration of five  $10^6$  load cycles.
- Calculation of the fatigue limit for  $N=5 \cdot 10^6$  load cycles
- The fatigue resistance that is supplied together with the mechanical characteristics of a material is the  $\sigma_{LA}$  fatigue limit supplied for a duration of  $10^7$  cycles.
- This value must then be recalculated taking into account the duration of  $5 \cdot 10^6$  cycles.
- The dependence of the fatigue load limits on the number of cycles can be expressed by the Wöhler equation below (Equation f-1):

$$\sigma_a^c \cdot N_a = \sigma_b^c \cdot N_b$$

- This relation is valid in correspondence of the following interval of  $100 < N < 10^7$  cycles.

The  $c$  constant is calculated by considering a breaking strength of  $\sigma = 0.95 R$  at  $N=100$  cycles. The solving of the equation f-1 with respect to the  $c$  parameter, obtains:

$$c = (\log_{10} 10^7 - \log_{10} 100) / (\log_{10} 0.95 R) - \log_{10} \sigma_{LA}$$

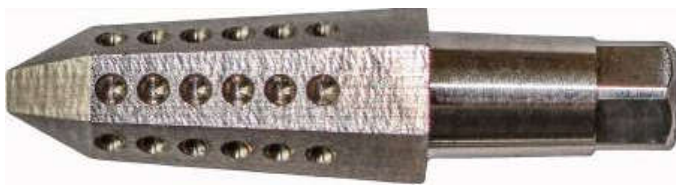
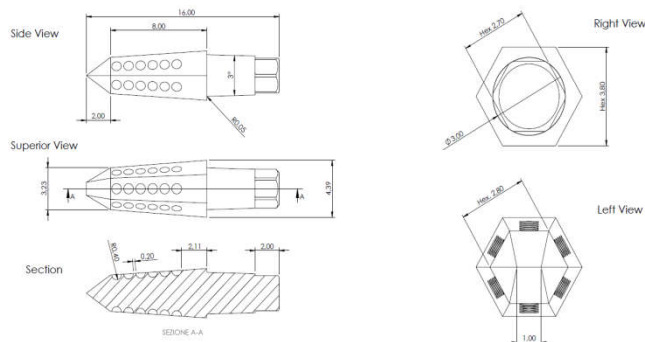
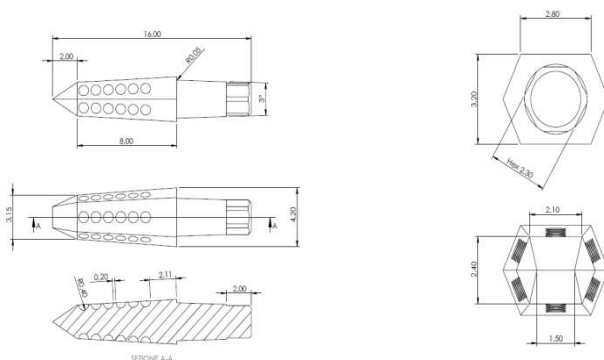
- Once  $c$  is known, the fatigue limit at  $N=5 \cdot 10^6$  cycles can then be calculated:

$$\sigma_{(L, 5 \cdot 10^6)} = \sigma_{(L, 10^7)} \cdot (10^7 / 5 \cdot 10^6)^{1/c}$$

- The fatigue limits calculated do not need to be multiplied by additional corrective factors given the surface finish and resistance to corrosion of the materials used.

### Test criteria adopted

The fatigue resistance test of the implant is conducted by applying the Sines resistance criteria, which are valid in case of triaxial stress conditions. These criteria are reliable when there are any changes in the direction of the principal stresses and when there are any wide of plasticization.

**Figure 8. RHPP Implant****Figure 9. IHPP Implant****Figure 10. RHPP Implant Dimensional Specifications****Figure 11. IHPP Implant Dimensional Specifications**

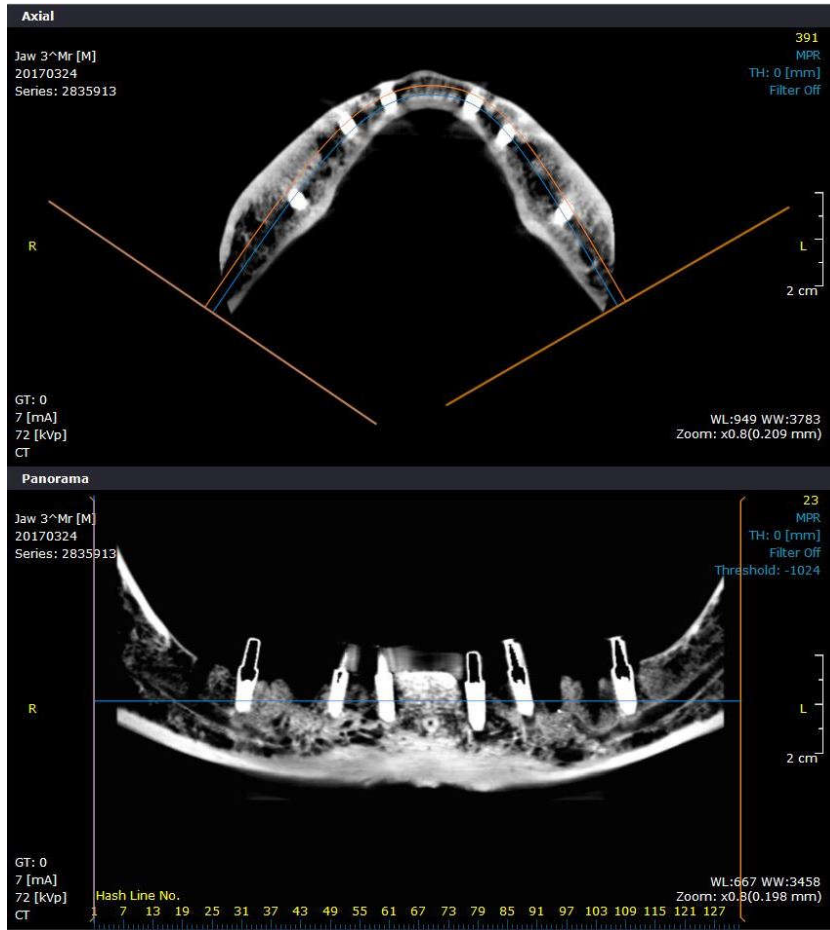


Figure 13. Anatomical Landmarks: IHPP Group Post-Op Analysis



Figure 14. Anatomical Landmarks: RHPP Group Post-Op Analysis



Figure 15. Mandible Specimens: IHPP group (Left) and RHPP group (Right) Post-Op



Figure 16. Extraction

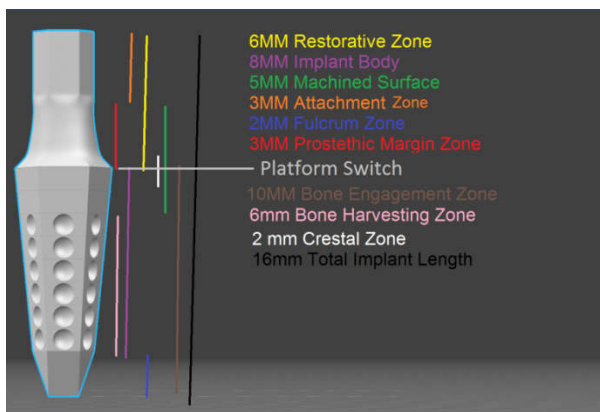


Figure 17. Prototype Zones

The test is conducted by comparing a conventional stress value, which we define as  $\sigma_{ALT}$ , with the correct fatigue limit value to consider a cycle ratio of  $R = -1$ . This correct fatigue limit will be indicated with  $\sigma_{AMM}$ .

This is followed by the definition of the two magnitudes defined above:

$$\sigma_{ALT} = (\sigma_{1a}^2 + \sigma_{2a}^2 + \sigma_{3a}^2 - \sigma_{1a} \cdot \sigma_{2a} - \sigma_{1a} \cdot \sigma_{3a} - \sigma_{2a} \cdot \sigma_{3a})^{1/2}$$

$$\sigma_{AMM} = \sigma_{(L,5 \cdot 10^6)} - k \cdot (\sigma_{1m} + \sigma_{2m} + \sigma_{3m})$$

The fatigue load limit of the implant meets the following condition:

$$\sigma_{ALT} = \sigma_{AMM}$$

Result of the static resistance structural tests:

Below are a series of illustrations showing the stress condition of the IHPPs and RHPP implants. In alphabetical order, the conditions represent:

- a) Von Mises equivalent stresses on the external threading of the BEZ and RZ.
- b) Equivalent Von Mises stresses on the implant.
- c) Detail of Von Mises equivalent stresses on the implant.
- d) Equivalent Von Mises stresses on the implant.
- e) Detail of Von Mises equivalent stresses on the implant.

**Result of the fatigue resistance structural tests**

The fatigue load limit was calculated by applying the procedure described earlier. The results that emerged are shown in the table below. It illustrates the fatigue load limit for each implant configuration, setting a limit value of nodes that does not exceed 0.5% and 5% of the total.

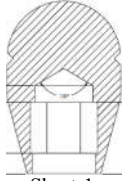
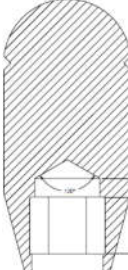
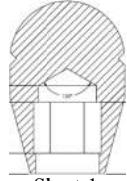
**Perio Test**

The Restorative Zone of (RZ) of the RHPP and IHPP were subjected to periotest to assess the mobility of the implant after insertion and subsequently the quality of their initial stability. A Periotest M handpiece, type 3218 by Medizintechnik Gulden e.K., was used, which measures the damping characteristics of the periodontium and, indirectly, tooth/implant mobility. During a measuring cycle of this device, an electrical motor activated a percussing rod to tap an implant surface approximately 16 times over a period of 4 seconds. It output measurements in the form of a Periotest Value (PTV) ranging from -8.0 to +50.0, which correlate to Miller’s Mobility Index (Table 7). The smaller the PTV, the higher is the stability of the implant. Table 8 illustrates the PTV and its interpretations in correlation to implant mobility clinically, according to the manufacturer guideline values. The device was held buccally in a horizontal position, +/- 25°, and directed perpendicularly to the long access of the implants at a distance between 0.6 and 2.5 millimeters to the center of the RZ end tip. The PTVs were taken three times for each implant and the average value was recorded. Additionally, the positions of placements were divided into Anterior and Posterior position in respect to D4 and D3 bone zone, for which the total average value was calculated individually for further analysis.

**RESULTS AND DISCUSSION**

The present in-vitro study analyzed thirty titanium, solid, 1P, threadless, and cross-sectionally hexagonal implant design during and after insertion. During delivery, the biomechanics and protocol facilitation aspects of the device, which utilized the concepts of fulcrum-lever force dissipation and wedging circumferentially and apically, were assessed, while the quality of initial stability and fixation was evaluated after. Engineered and intended for immediate loading, the implants were delivered into two human mandibles D1 bone zones by means of conventional rotational, impact, and hybrid methods.

Table 3. Testing Conditions of each implant configuration test

Implants	IHPP Conf. 1	IHPP Conf. 2	IHPP Conf. 3	IHPP Conf. 4	RHPP Conf. 5
Coping attachment design	 Short-1	 Long-1	 Long-2	 Short-1	 Short-2
RZ coverage	2.5mm	5mm	2.5mm	5mm	2.5mm
BEZ coverage (BIC%)	7mm (70%)	7mm (70%)	10mm (100%)	7mm (70%)	7mm (70%)
Load direction in respect to FZ	Parallel	Parallel	Parallel	Perpendicular	Parallel

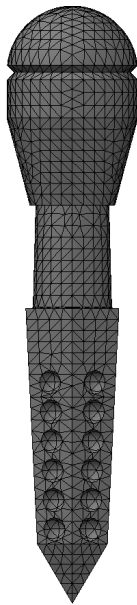


Figure 18. IHPP Implant Configuration 1 test with support – Mesh of the mathematical model with tetrahedral elements

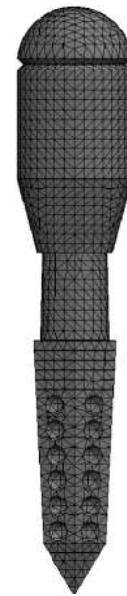


Figure 20. IHPP Implant Configuration 3 test with support – Mesh of the mathematical model with tetrahedral elements

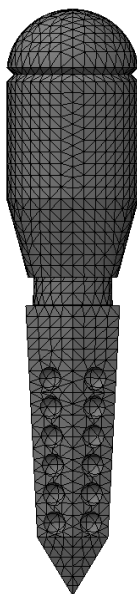


Figure 19. IHPP Implant Configuration 2 test with support – Mesh of the mathematical model with tetrahedral elements

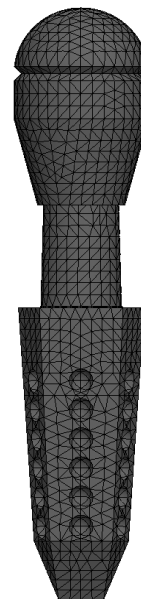


Figure 21. IHPP Implant Configuration 4 test with support – Mesh of the mathematical model with tetrahedral elements.

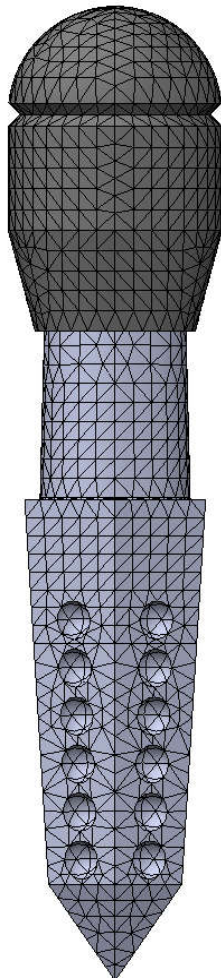


Figure 22. RHPP Implant Configuration 5 test with support – Mesh of the mathematical model with tetrahedral elements

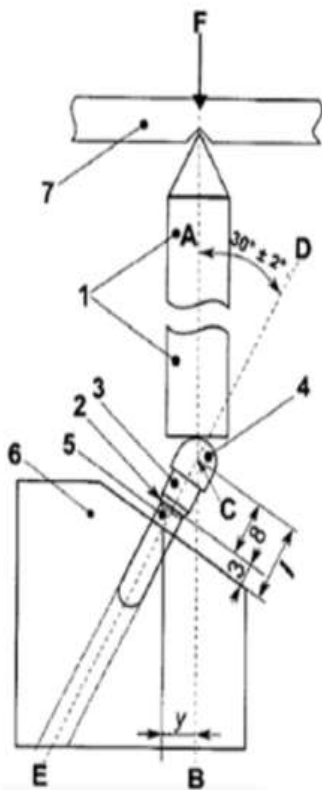


Figure 23. Test scheme indicated by the UNI EN ISO 14801:2017

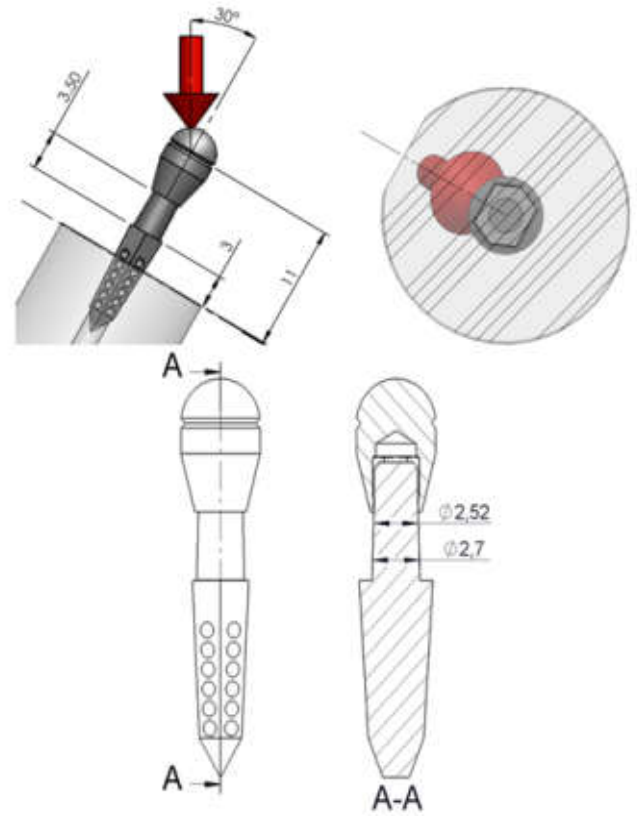


Figure 24. IHPP Implant Configuration 1 test with support – Main dimensions for the structural analysis (Dimensions in millimeters)

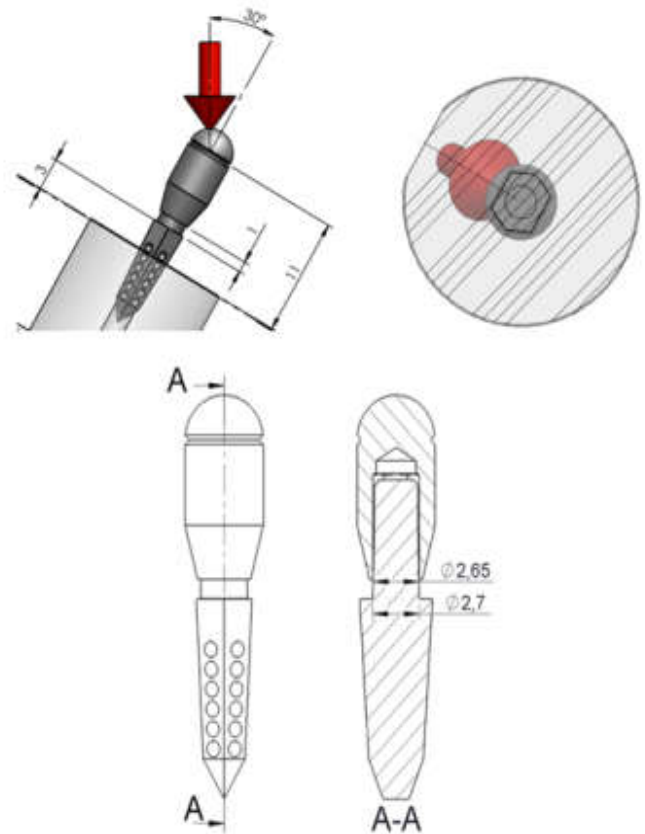


Figure 25. IHPP Implant Configuration 2 test with support – Main dimensions for the structural analysis (Dimensions in millimeters)

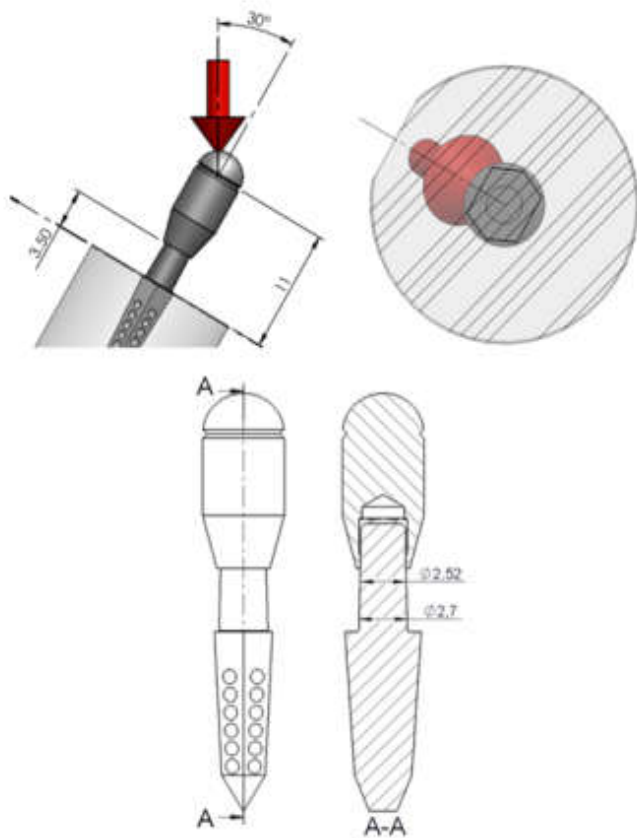


Figure 26. IHPP Implant Configuration 3 test with support – Main dimensions for the structural analysis (Dimensions in millimeters)

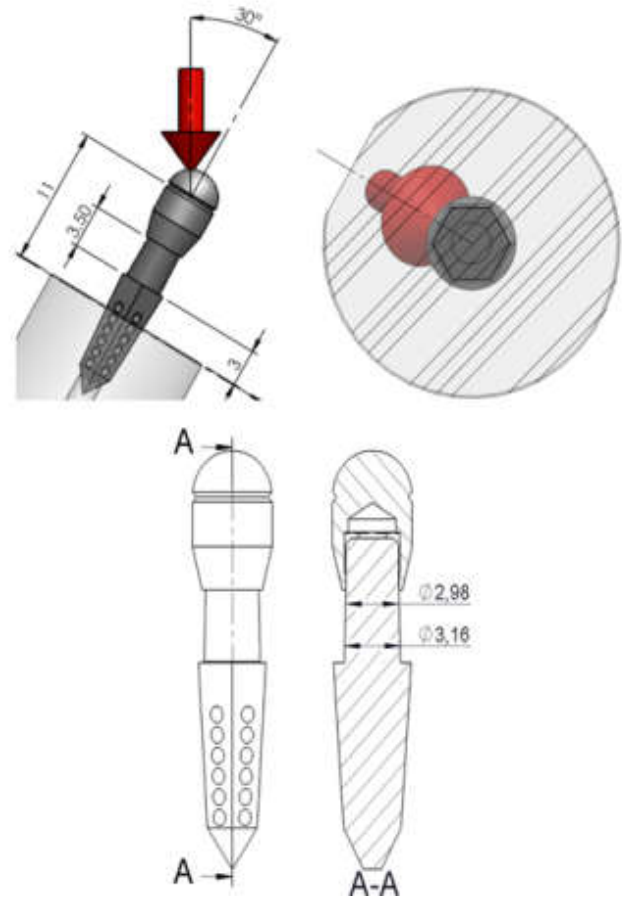


Figure 28. RHPP Implant Configuration 5 test with support – Main dimensions for the structural analysis (Dimensions in millimeters)

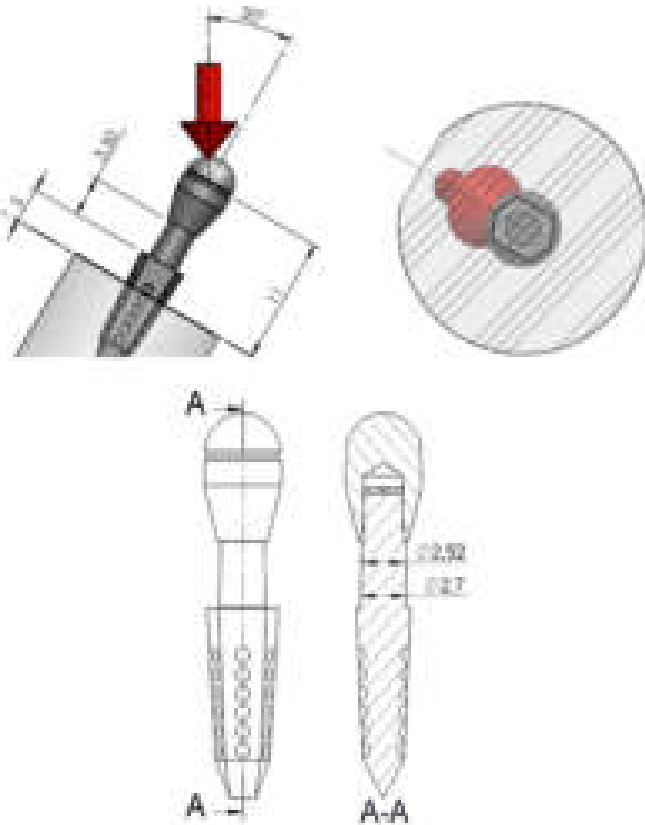


Figure 27. IHPP Implant Configuration 4 test with support – Main dimensions for the structural analysis (Dimensions in millimeters)

Table 4. Composition of the implant components

Component	Material	c	$\sigma_{(L,5 \cdot 10^6)}$ [MPa]	$k=\sigma_{(L,5 \cdot 10^6)}/R$
BEZ	Titanium Gr. 4	55.74	430.31	0.7824
RZ & Coping	Titanium Gr. 5	11.49	318.65	0.3705

Table 5. Mechanical properties of the material used

Element type		BEZ	RZ & Coping
Material		Gr. 4	Ti-6Al-4V Gr. 5
Properties of the material	Modulus of elasticity [GPa]	110	110
	Poisson's ratio	0.34	0.34
	Breaking strength [MPa]	550	860
	Yield strength [MPa]	480	790
	Elongation at break %	15	15
	Fatigue resistance LA [MPa] per 1·10 <sup>7</sup> cycles	425	300

Table 6. Fatigue load limits for each implant with 0.5% and 5% limit value of nodes

Implant with support	Fatigue load limit per N=5·10 <sup>6</sup> [N]	
	With maximum percentage of nodes outside the test = 0.5%	With maximum percentage of nodes outside the test = 5%
	IHPP Config. 1 test	273
IHPP Config. 2 test	276	605
IHPP Config. 3 test	196	404
IHPP Config. 4 test	281	577
RHPP Config. 5 test	374	767

**Table 7. PTVs compared with Miller Mobility Index**

Miller index	Clinical Finding	Periosteal Value
0	No discernable movement	-8.0 to +9.0
1	Palpable movement	+10 to +19
2	Obvious movement	+20 to +29
3	Movement on tip pressure	+30 to +50

**Table 8. Guideline values in correlation to PTV**

Values	Mobility interpretation
-8.0 to 0.0	Good osseointegration; the implant can be loaded
+0.1 to +9.9	Clinical examination is required; loading of the implant might or might not be possible, depending on implant type and clinical situation
+10.0 or higher	Osseointegration is insufficient, the implant cannot be loaded

**Table 9. The mean PTVs of all the implants**

Group 1: 15 RHPP		Group 2: 15 IHPP	
8 RHPP Rotational	7 RHPP Hybrid Method	Impact Method	
Anterior	-6.4	-6.3	-6.4
Placement	-6.1	-5.8	-4.7
D1	-6.6	-7.1	-4.2
	-5.2	-5.5	-5.1
Average D1	-6.075	-7.05	-6.175
Posterior	-5.4	-6.5	-4.9
placement	-3.7	-5.9	-3.9
D2	-4.3	-6.1	-5.2
	-4.2	-3.6	-3.8
Average D2	-4.4	-6.16	-4.4
		-4.4	-3.4

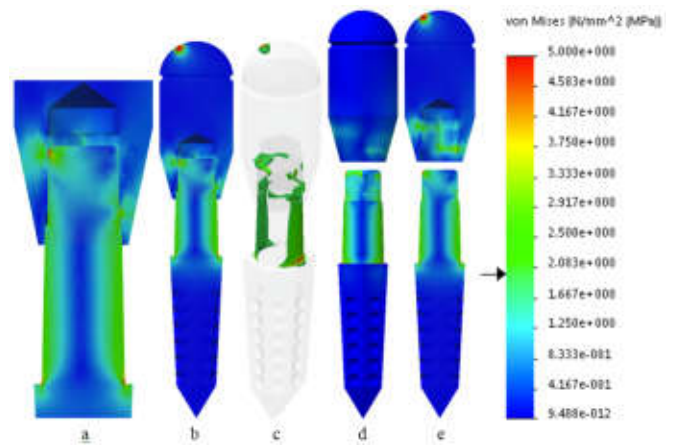


**Figure 31.**

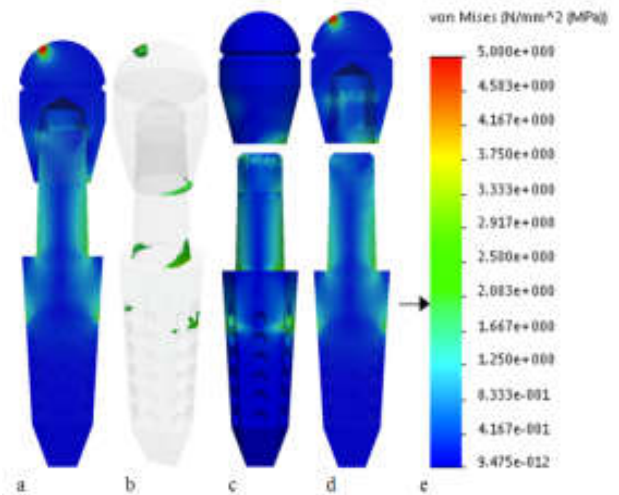


**Figure 32.**

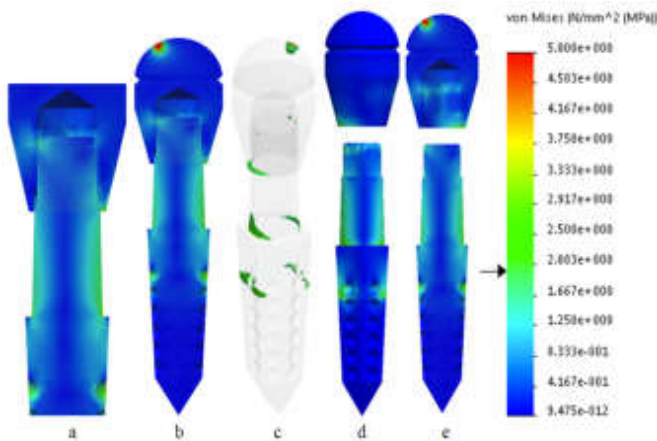


**Figure 29.**

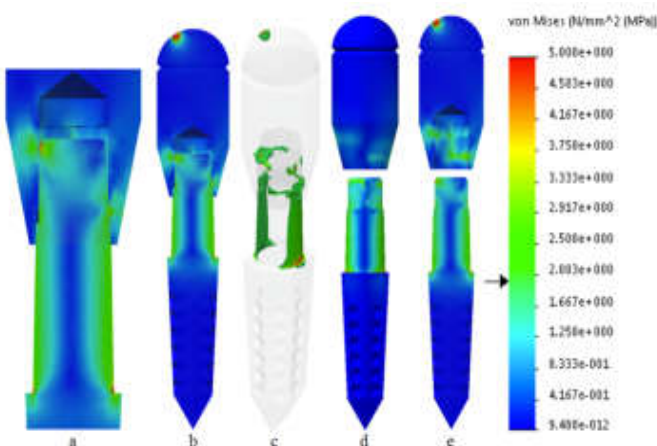


**Figure 30.**

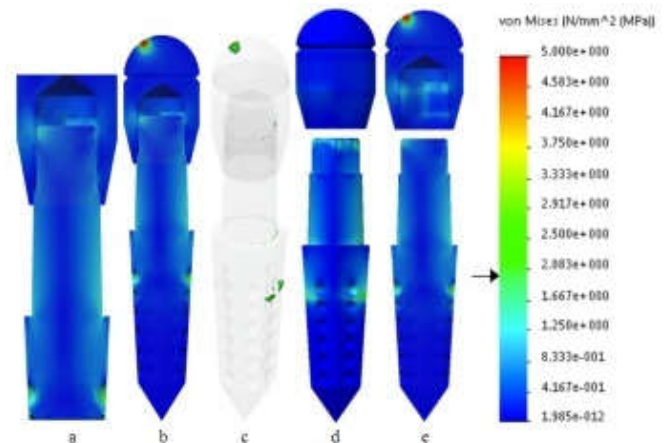


**Figure 33.**

The concept of osseointegration has come a long way since Brånemark introduced in the 1970's. Ever since, geometric designs and surface characteristics have been continuously modified and incorporated into varieties of implant designs for the sole purpose of achieving initial stability. How bone and implant interact essentially defines the long-term success in implant surgery. Profound osseointegration depends on the quality of initial rigid fixation at the time of implant placement, primary stability, and bone apposition onto implant surface during and after the healing process, secondary stability.<sup>85</sup> On the other hand, biomechanical factors

implemented in implant designs and prude treatment planning demand close considerations to minimize the potential risks of failure. Having the mentioned criteria in mind, recently we have designed a unique 1P implant system to provide for enhanced initial stability, conservative osteotomy, and controlled ridge expansion. Inspired by an industrial chisel, our 1P implant can be easily differentiated by its shape and design, when compared to other common implant systems. The polygon design, hexagonal in cross-section, delivers six slightly rounded line angles and flat planes with six semi-spherical indentations on each. These macrogeometries are present from the Crestal Zone (CZ) and are continuous along the tapering Bone Engagement Zone (BEZ) to finally merge together at the Fulcrum Zone (FZ) creating a miniature chisel. The objective behind such design was to produce a facilitating effect during and an antirotational effect after implant insertion within the osteotomy via harvesting the power of fulcrum-lever and wedging concept. The FZ, a V-shaped tip coupled with a pair of auxiliary flat planes on either ends, stands as the primary wedge, anchorage, and fulcrum. Together with the tapering BEZ, the lever and the secondary wedge, they act harmoniously effective to decrease amount of load necessary to insert the implant into osteotomy.<sup>84</sup> During implant placement, this design allows operators to press-fit and/or rotate and guide the implant into freshly extracted socket or prepared osteotomy with enhanced control. Taking both the threadless and tapered design into account, a 1P design provides ease of implementation, in terms of fewer protocol steps and accessibility, and prevents inadvertent bone loss that the threaded implants may cause during insertion into the hard to reach D3 and D4.<sup>27</sup> In comparison to parallel-walled implants, previous studies have confirmed that tapered designs offer enhanced initial stability, particularly in bone types of soft quality, due to higher compressive force on the cortical bone regions.<sup>57,58,85,86</sup> These findings were confirmed in this clinical study as none of the prototypes exhibited micromovement that may held accountable for poor initial stability.

The implant is designed to serve as an exceptional anti-rotational lock. Twelve flat planes of the BEZ and FZ with different areas and angulations appose bone surface and direct bone remodeling and growth creating an accurate negative impression of the implant, as compression loads, by which rotational load is resisted during parafunctional activities.<sup>84</sup> The crestal bone had conformed precisely to the CZ circumference without any evident gaps clinically. The corners were embedded into cortical bone rendering rotational movement impossible. Close approximation of bone-implant at the CZ seals the entrance of fibrous tissue and pathogens at early stage of healing and enhances initial stability.<sup>84,87,88</sup> Two studies<sup>88,90</sup> have reported an angled geometry at the crest module of a design reduces the risks of bone resorption via imposing compressive component to adjacent bone. Additionally, it is hypothesized that such tapering design prevents surgical complications such as dislodgement into facial cavities. Whereas other common implant systems may have only a few spherical indentations, the Bone Harvesting Zone (BHZ) holds a total of thirty-six along the BEZ that transfer occlusal load into the bone and resist strain and stress.<sup>84</sup> It was discovered in our study that these indentations also served as reservoirs of autogenous bone harvested during insertion. Aside from their intended purpose, the BEZ and FZ macrogeometries shaved the osteotomy wall and produced autogenous bone while the implant was being seated

rotationally. Significant amount of bone particles were harvested and collected during all three delivery methods by which the need for bone graft could potentially be decrease. In conjunction with precise bone-implant contact, bone-harvesting capability of this design promotes profound initial stability during bone healing and aid subsequent long-term fixation.

In the 1P implant systems, the prosthetic abutment and implant body are milled as one single unit. A prosthetic crown may be retained on the abutment portion either by a screw or cement.<sup>27</sup> The screw-retained crowns (SRC) are most common due to retrievability and inconsequential retention and resistance-form.<sup>91,92</sup> Although SRC have been the most popular choice, studies have reported that an inclination is on the rise towards cement-retained crowns (CRC).<sup>92,93</sup> In natural tooth restorations, the type of luting agent mandates the quality of resistance to dislodgment under compressive and shear forces.<sup>91</sup> Rosenthal *et al*<sup>94</sup> proved high compressive strength cements are the best candidates to counter such forces thereby applicable for implant-supported crowns. The hex abutment design observes the same retention and resistance-form as natural tooth preparation. In despite of proportionally smaller surface areas, the parallel walls and angled-hexed designs can accommodate dimensionally larger crowns than natural tooth preparations.<sup>95,96</sup> In another study, Kwan *et al*<sup>91</sup> demonstrated that CRCs of common hex abutment designs well-resisted displacement under off-axial load, which mimics physiologic load. The other possible cause of affinity towards the traditional CRC is the possible structural drawbacks of the screw system. A SRC adds an additional screw to the 2P systems screw collection, abutment and healing screw, tallying to three. Although recent screw designs and concepts have reduced the rate of screw failure in the 2P designs dramatically,<sup>47</sup> the resultant complications call its value into question. On the other hand, the screw-less CRC 1P implant conveniences both operators and patients as the hex abutment provides for the prosthetic crown attachment and eliminates possible uncover surgery.

Load distribution is greatly influenced by multiple aspects of the implant, bone, and force vectors. Finite Element Analysis (FEA) was designed in the late 1970's to predict functionality and feasibility of different implant designs in laboratory settings and predict their behavior and effects in real-life clinical cases. Therefore, some margin of error accompanies such theoretical analysis.<sup>8</sup> In this in-vitro study, the results of FEA were divided into the BEZ, the fixture, and the RZ, the abutment. Four types of titanium alloy attachments were used that slightly differed in vertical height and the amount of the RZ they covered. Efforts were made to stimulate realistic clinical scenarios as closely as possible by designing multiple implant configuration tests. In static resistance structural test, the implant configurations 1, 2, 4, and 5 tests demonstrated even load distribution vertically and laterally through out the RZ and the initial 1/3 of the BEZ, so that the load was completely dissipated and neutralized before reaching the embedded 2/3 of the BEZ (Figure 15, 16, 18, 19). In the mentioned configuration tests, the Von Mises equivalent stress never exceeded beyond 2.083e. The epicenters were at spherical head-RZ, RZ-BEZ, and BEZ-Base interfaces. IHPP implant configuration tests experienced identical load distribution patterns with almost similar stress resistance magnitudes. It was assumed that the minimal difference was due to the difference in the design of titanium coping

attachment, which provided stability and support in resisting load. Therefore, the same principle might be duplicable clinically. The more embodiment of the RZ by prosthesis, the more occlusal load resisted and less transferred to the crestal bone. However, in IHPP implant configuration 3, where the BEZ was fully embedded, major stress of 4.583e was experienced at the BEZ-RZ interface diagonally opposite of load application area. A possible explanation could be a combination of the design of this interface, which is near butt joint, and higher bending movement aided by the least stable coping. In this particular scenario, the base and the BEZ-RZ interface were equi-level while the load source and the platform switch were the furthest apart when compared to other configuration tests. The long coping that covered the minimum amount of the RZ collaboratively provided longer moment of arm and consequently more bending movement. Additionally, load application parallel or perpendicular to the FZ tip did not make significant difference in terms of fatigue load limit, load dissipation pattern, and stress resistance tolerance in IHPP implant configuration 1 and 4.

In fatigue load and structural static resistance tests, RHPP implant configuration 5 test with a short coping demonstrated the best result (Figure 19 and table 6). It tolerated 374-N with 0.5% and 767-N with 5% maximum nodes outside of the test. Load distribution pattern was much more spread uniformly, while the epicenters located at RZ-BEZ and BEZ-Base interfaces. Although the over-all magnitude of stress equaled the other configuration tests, the area under the most stress was significantly the smallest in the RHPP configuration 5 test. The greatest constrain related to BEZ-Base interface at the level of first spherical indentation of the BEZ. The methods for assessing implant mobility or stability are either subjective or objective. An objective evaluation becomes highly important when examiner-dependent nature of the subjective method may be convoluted by bias.<sup>98</sup> Periotest is a quantitative, noninvasive, and reproducible method that has been reported reliable to evaluate primary stability of implant upon delivery.<sup>99-102</sup> In this study, periotest device measured impressive PTVs consistently from -7.5 to -2.9 as the most to least stable implant (Table 8). The placements were divided into anterior and posterior in respect to their mandibular position. The average PTV of anterior position group was determined greater than their posterior counterpart. The highest values on average belonged to Group 1 Hybrid method, RHPP implants. Additionally, our evaluation during extraction determined that the polygon implant provided sturdy primary stability within D1 and D2 bone when industrial plier had to be used often.

A major limitation of this study, however, was the small sample size of implants examined. Prospective clinical research is needed to determine the exact micromovement and heat generation statistical figures as well as the long-term effects of load distribution around implants and abutments in respect to marginal bone preservation.

## Conclusion

### Within limitations of this study, we demonstrated that:

- 1) A polygon-shaped (in-cross section) and tapered design enhances initial stability and provides for anti-rotational lock.

- 2) Fulcrum-Levered force dissipation concept facilitates and simplifies common protocols in implantology.
- 3) The conical design prevents dislodgement into oral cavities.
- 4) Over all design provides clinicians with enhanced control and maneuverability during insertion.

## Disclosure

The authors have no financial interest in any of the companies mentioned in this article and received no compensation for writing this article. For this work, no funding was received.

## Approval

For this ex-vivo study, neither approval from an institutional review board nor an ethics review committee was necessary.

## REFERENCES

1. Powers, JM. and Sakaguchi RJ. 2006. Cements. In: J.M. Powers and R.J. Sakaguchi (Eds), *Craig's Restorative Dental Materials* (pp. 481). 12<sup>th</sup> ed., MO, St. Louis: Mosby Elsevier.
2. Ring ME. 1995. Pause for a moment in dental history. A Thousand Years of Dental Implants: A Definitive History: Part 1. *Compend Contin Educ Dent.*, 16:1060-1069.
3. Albrektsson T, Brånemark PI, Hansson HA, *et al.* 1981. Osseointegrated titanium implants. Requirements for ensuring a long-lasting, direct bone-to-implant anchorage in man. *Acta Orthop Scand.*, 52:155-170.
4. Parel SM, Schow SR. 2005. Early clinical experience with a new one-piece implant system in single tooth sites. *J Oral Maxillofac Surg.*, 63(suppl 2):2-10.
5. Hahn J. 2005. One-piece root-form implants: a return to simplicity. *J Oral Implantol.*, 31:77-84.
6. Hahn JA. 2007. Clinical and radiographic evaluation of one-piece implants used for immediate function. *J Oral Implantol.*, 33:152-155.
7. Ostman PO, Hellman M, Albrektsson T, Sennerby L. 2007. Direct loading of Nobel Direct and Nobel Perfect one-piece implants: a 1-year prospective clinical and radiographic study. *Clin Oral Implants Res.*, 18: 409-418.
8. Ormianer Z, Ben AA, Duda M, *et al.* 2012. Stress and Strain Patterns of 1-Piece and 2-Piece Implant Systems in Bone: A 3-Dimensional Finite Element Analysis. *Implant Dent.*, 21(3): 225-229.
9. Albrektsson T, Wennerberg A. 2005. The impact of oral implants: past and future, 1966-2042. *J Can Dent Assoc.*, 71:327.
10. Jokstad A, Carr AB. 2007. What is the effect on outcomes of time-to-loading of a fixed or removable prosthesis placed in implant(s)? *Int J Oral Maxillofac Implants.*, 22:19-48.
11. Avila G, Galindo P, Rios H, *et al.* 2007. Immediate implant loading: Current status from available literature. *Implant Dent.*, 16:235-245.
12. Del Fabbro M, Testori T, Francetti L, *et al.* 2006. Systematic review of survival rates for immediately loaded dental implants. *Int J Periodontics Restorative Dent.*, 26: 249-263.
13. Ioannidou E, Doufexi A. 2005. Does loading time affect implant survival? A meta-analysis of 1,266 implants. *J Periodontol.*, 76:1252-1258.

14. Attard NJ, Zarb GA. 2005. Immediate and early implant loading protocols: A literature review of clinical studies. *J Prosthet Dent.*, 94:242–258.
15. Gapski R, Wang HL, Mascarenhas P, et al. 2003. Critical review of immediate implant loading. *Clin Oral Impl Res.*, 14: 515–527.
16. Testori T, Smukler-Moncler S, Francetti L, et al. 2001. The immediate-loading of Osseotite implants. A clinical and histologic assessment 4 months after being brought into function. *Parodontie-Dentisterie Restauratrice*, 21:451–459.
17. Degidi M, Scarano A, Iezzi G, et al. 2003. Periimplant bone in immediately loaded titanium implants: histologic and histomorphometric evaluation in human. A report of two cases. *Clin Implant Dent Related Res.*, 5:170–175.
18. Vogel RE, Davliakos JP. 2002. Spline implant prospective multicenter study: Interim report on prosthetic screw stability in partially edentulous patients. *J Esthet Re- stor Dent.*, 14:225–237.
19. Broggin N, McManus LM, Hermann JS, et al. 2003. Persistent acute inflammation at the implant-abutment interface. *J Dent Res.*, 82:232–237.
20. Jones AA, Cochran DL. 2006. Consequences of implant design. *Dent Clin N Am.*, 50:339–360.
21. Prithviraj DR, Gupta V, Muley N, et al. 2013. One-piece implants: Placement timing, surgical technique, loading protocol, and marginal bone loss. *J Prosthodont.*, 22:237–244.
22. Laney WR, Broggin N, Buser D, et al, eds. 2007. Glossary of Oral and Maxillofacial Implants. Hanover Park, IL: Quintessence; 1127.
23. Piattelli A, Corigliano M, Scarano A, et al. 1997. Bone reactions to early occlusal loading of two-stage titanium plasma-sprayed implants: a pilot study in monkeys. *Int J Periodontics Restorative Dent.* 17: 162–169.
24. Piattelli A, Corigliano M, Scarano A, et al. 1998. Immediate loading of titanium plasma-sprayed implants: an histologic analysis in monkeys. *J Periodontol.*, 69:321-327.
25. Piattelli A, Ruggeri A, Franchi M, et al. 1993. An histologic and histomorphometric study of bone reactions to unloaded and loaded non-submerged single implants in monkeys: a pilot study. *J Oral Implantol.* 19:314-320.
26. Albrektsson T, Lekholm U. 1989. Osseointegration: Current state of the art. *Dent Clin North Am.*, 33:537-554
27. Misch, CE 2008. Rationale for Implants: Generic root form component terminology. In: Misch, CE (eds.), *Contemporary Implant Dentistry* (pp. 26-37). 3<sup>rd</sup> ed., MO, St. Louis: Mosby Elsevier.
28. Swart LC, van Niekerk DJ. 2008. Simplifying the implant treatment for an unrestorable premolar with a one-piece implant: A clinical report. *J Prosthet Dent.*, 100:81-85.
29. Misch, CE. 2015. Clinical Biomechanics in Implant Dentistry. In: Misch CE, Bidez MW (eds.), *Dental Implant Prosthetics* (pp.95- 106). 2nd ed., MO, St. Louis: Mosby Elsevier.
30. Yadav RS, Sangur R, Mahajan T, et al. 2015. An Alternative to Conventional Dental Implants: Basal Implants. *Rama Univ J Dent Sci.* 2(2):22-28.
31. Misch, CE. 2015. An Implant Is Not a Tooth: A Comparison of Periodontal Indices. In: Misch CE, Strong JT, Bidez MW (eds.), *Dental Implant Prosthetics* (pp.46-65). 2nd ed., MO, St. Louis: Mosby Elsevier.
32. Vacek JS, Gher ME, Assad DA, et al. 1994. The dimensions of the human Dentogingival junction. *Int J Periodontics Restorative Dent.*, 14:155-165.
33. Vela NX, Rodríguez CX, Rodado AC, Segala` TM. 2006. Benefits of an Implant Platform Modification Technique to Reduce Crestal Bone Resorption. *Implant Dent.*, (15):313-320.
34. Tarnow DP, Cho SC, Wallace SS. 2000. The effect of inter-implant distance on the height of inter-implant bone crest. *J Periodontol.*, 71:546-549.
35. Hartman GA. 2004. Initial implant position determines the magnitude of crestal bone remodeling. *J Periodontol.*, 74:572-577.
36. Gadhia MH, Holt RL. 2003. A new implant design for optimal esthetics and retention of interproximal papillae. *Implant Dent.*, 12:164-169.
37. Hermann JS, Buser D, Schenk RK, et al. 2001. Biologic width around one- and two-piece titanium implants. A histometric evaluation of unloaded nonsubmerged and submerged implants in the canine mandible. *Clin Oral Implants Res.*, 12:559-571.
38. Hermann JS, Cochran DL, Nummikoski PV, et al. 1997. Crestal bone changes around titanium implants. A radiographic evaluation of unloaded nonsubmerged and submerged implants in the canine mandible. *J Periodontol.*, 68:1117-1130.
39. Lekholm U, Ericsson I, Adell R, et al. 1986. The condition of the soft tissues t tooth and fixture abutments supporting fixed bridges. A microbiological and histological study. *J Clin Periodontol.*, 13:558-562.
40. Piattelli A, Vrespa G, Petrone G, et al. 2003. Role of the microgap between implant and abutment: A retrospective histologic evaluation in monkeys. *J Periodontol.*, 74:346-352.
41. Hermann JS, Schoolfield JD, Schenk RK, et al. 2001. Influence of the size of the microgap on crestal bone changes around titanium implants. A histometric evaluation of unloaded non-submerged implants in the canine mandible. *J Periodontol.*, 2:1372-1383.
42. Kazemi M, Jalali H, Egtehari M, et al. 2012. Acrylic resin polymerization in direct contact to the abutment and the temperature at the bone-implant interface: a pilot in vitro study. *J Oral Implantol.*, 38:595-601.
43. Carrio CP, Ferrin LM, Oltra DP, et al. 2011. Risk factors associated with early failure of dental implants: a literature review. *Med Oral Patol Oral Cir Bucal.*, 16:514-517.
44. Eriksson A, Albrektsson T, Grane B, et al. 1982. Thermal injury to bone. A vital-microscopic description of heat effects. *Int J Oral Surg.*, 11:115–121.
45. Matthews LS, Hirsh C. 1972. Temperatures measured in human cortical bone when drilling. *J Bone Joint Surg Am.*, 54:297–308.
46. Haider R, Watzek G, Plenck H. 1993. Effects of drill cooling and bone structure on IMZ implant fixation. *Int J Oral Maxillofac Implants*, 8:83–91.
47. Misch, CE. 2015. Stress Treatment Theorem for Implant Dentistry: The key to implant Treatment Plans. In: Misch, CE (eds.), *Dental Implant Prosthetics* (pp.159- 192). 2nd ed., MO, St. Louis: Mosby Elsevier.
48. Okayasu K, Wang HL. 2011. Decision tree for the management of peri-implant diseases. *Implant Dent.*, 20: 256-261.

49. Omer C, Eran G, Machtei EE. 2010. Cooling Profile Following Prosthetic Preparation of 1-Piece Dental Implants. *Journal of Oral Implantology*, 36(4): 273-279.
50. Gross M, Laufer BZ, Ormianar Z. 1995. An investigation on heat transfer to the implant-bone interface due to abutment preparation with high-speed cutting instruments. *Int J Oral Maxillofac Implants.*, 10:207-212.
51. Siegele D, Soltesz U. 1989. Numerical investigations of the influence of implant shape on stress distribution in the jaw bone. *Int J Oral Maxillofac Implants*, 4:333-340.
52. Chun HJ, Cheong SY, Han JH, et al. 2002. Evaluation of design parameters of osseointegrated dental implants using finite element analysis. *J Oral Rehabil.*, 29:565-574.
53. Binon PP. 2000. Implants and components: Entering the new millennium. *Int J Oral Maxillofac Implants*, 15:76-94.
54. Cehreli MC, Akça K, Iplikcioglu H. 2004. Force transmission of one- and two-piece morse-taper oral implants: A nonlinear finite element analysis. *Clin Oral Implants Res.*, 15:481-489.
55. Van Oosterwyck H, Duyck J, Vander Sloten J, et al. 1998. The influence of bone mechanical properties and implant fixation upon bone loading around oral implants. *Clin Oral Implants Res.*, 9:407-418.
56. Maiorana C, Santoro F. 2002. Maxillary and mandibular bone reconstruction with hip grafts and implants using Frialit-2 implants. *Int J Periodontics Restorative Dent.*, 22:221-229.
57. O'Sullivan D, Sennerby L, Meredith N. 2004. Influence of implant taper on the primary and secondary stability of osseointegrated titanium implants. *Clin Oral Implants Res.*, 15:474-480.
58. O'Sullivan D, Sennerby L, Meredith N. 2000. Measurements comparing the initial stability of five designs of dental implants: A human cadaver study. *Clin Implant Dent Relat Res.*, 2:85-92.
59. Kim JW, Baek SH, Kim TW, et al. 2008. Comparison of stability between cylindrical and conical type mini-implants: Mechanical and histological properties. *Angle Orthod.*, 78:692-698.
60. Martinez H, Davarpanah M, Missika P, et al. 2001. Optimal implant stabilization in low density bone. *Clin Oral Implants Res.*, 12:423-432.
61. Ivanoff CJ, Grondahl K, Bergstrom C, et al. 2000. Influence of bicortical or monocortical anchorage on maxillary implant stability: A 15-year retrospective study of Branemark System implants. *Int J Oral Maxillofac Implants*, 15:103-110.
62. Romanos GE, Basha-Hijazi A, Gupta B, et al. 2014. Role of clinician's experience and implant design on implant stability. An ex vivo study in artificial soft bones. *Clin Implant Dent Relat Res.*, 16:166-171.
63. Romanos GE, Ciornei G, Jucan A, et al. 2014. In vitro assessment of primary stability of Straumann(R) implant designs. *Clin Implant Dent Relat Res.*, 16: 89-95.
64. Wilmes B, Ottenstreuer S, Su YY, et al. 2008. Impact of implant design on primary stability of orthodontic mini-implants. *J Orofac Orthop.*, 69:42-50.
65. Siegele D, Soltesz U. 1989. Numerical investigations of the influence of implant shape on stress distribution in the jaw bone. *Int J Oral Maxillofac Implants*, 4:333-340.
66. Olate S, Chaves Netto HD, Kluppel LE, et al. 2011. Mineralized tissue formation associated with 2 different dental implant designs: Histomorphometric analyses performed in dogs. *J Oral Implantol.*, 37:319-324.
67. Bothe RT, Beaton LE, Davenport HA. 1940. Reaction of bone to multiple metallic implants. *Surg Gynecol Obstet.*, 71:598-602.
68. Grandin HM, Berner S, Dard M. 2012. A Review of Titanium Zirconium (TiZr) Alloys for Use in Endosseous Dental Implants. *Materials*, 5:1348-1360.
69. Steinemann, S.G. 1998. Titanium: The material of choice? *Periodontology 2000*, 17:7-21.
70. Parr, G.R.; Gardner, L.K.; Toth, R.W. Titanium, 1985. The mystery metal of implant dentistry—Dental materials aspects. *J. Prosthet. Dent.*, 54, 410-414.
71. Naganawa, T, Ishihara Y, Iwata, T, et al. 2004. In vitro biocompatibility of a new titanium-29niobium-13 tantalum-4.6zirconium alloy with osteoblast-like MG63 cells. *J. Periodontol.*, 75, 1701-1707.
72. Bernhard N, Berner S, De Wild M, et al. 2009. The binary TiZr alloy: A newly developed Ti alloy for use in dental implants. *Forum Implantol.*, 5, 30-39.
73. Conner K, Sabatini R, Mealey B, et al. 2003. Guided bone regeneration around titanium plasma-sprayed, acid-etched and hydroxyapatite-coated implants in the canine model. *J Periodontol.*, 74:658-668.
74. Bhat V, S. Balaji SS. 2014. Surface Topography of dental implants. *Nitte University Journal of Health Science*, 4(4):46-54.
75. Brett PM, Harle J, Salih V, Mihoc R, Olsen I, Jones FH. 2004. Roughness response genes in osteoblasts. *Bone*, 35:124-133.
76. Buser, D. 2001. Titanium for dental applications (II): Implants with roughened surfaces. In Brunette D, Tengvall P, Textor, M, Thomson P (Eds.), *Titanium in Medicine* (pp. 232-239). Springer: Berlin, Germany.
77. Hansson S, Norton M. 1999. The relation between surface roughness and interfacial shear strength for bone-anchored implants. A mathematical model. *J Biomech.*, 32:829-836.
78. Testori T, Wiseman L, Woolfe S, Porter S. 2001. A prospective multicenter clinical study of the Osseotite implant: four-year interim report. *Int J Oral Maxillofac Implants*, 16:193-200.
79. Chuang SK, Tian L, Wei LJ, et al. 2001. Kaplan-Meier analysis of dental implant survival: A strategy for estimating survival with clustered observations. *J Dent Res.*, 80:2016-2020.
80. Shibuya Y, Takata N, Takeuchi J, et al. 2012. Analysis of the 619 Brånemark System TiUnite implants: A retrospective study. *Kobe J Med Sci.*, 58:E19-E28.
81. Baqain ZH, Moqbel WY, Sawair FA. 2012. Early dental implant failure: Risk factors. *Br J Oral Maxillofac Surg.*, 50:239-243.
82. Misch CE, Suzuki JB, Misch-Dietch FM et al. 2005. A positive correlation between occlusal trauma and peri-implant bone loss: literature support. *Implant Dent.*, 14:108-116.
83. Goto T. 2014. Osseointegration and dental implants [in Japanese]. *Clin Calcium.*, 24:265-271.
84. Misch, CE. 2015. Implant Treatment Planning: Scientific Rationale for Dental Implant Design. In: Misch CE, Strong JT, Bidez MW (eds.), *Dental Implant Prosthetics* (pp.26- 45). 2nd ed., MO, St. Louis: Mosby Elsevier.
85. Sakoh J, Wahlmann U, Stender E, et al. 2006. Primary stability of a conical implant and a hybrid, cylindrical

- screw-type implant in vitro. *Int J Oral Maxillofac Implants.*, 21:560-566.
86. Degidi M, Daprile G, Piattelli A, et al. 2007. Evaluation of factors influencing resonance frequency analysis values, at insertion surgery, of implants placed in sinus-augmented and non-grafted sites. *Clin Implant Dent Relat Res.*, 9:144-149.
  87. Esposito M, Thomsen P, Ericson LE, et al. 1999. Histopathologic observations on early oral implant failures. *Int J Oral Maxillofac Implants*, 14:798-810.
  88. Esposito M, Hirsch JM, Lekholm U, et al. 1998. Biological factors contributing to failures of osseointegrated oral implants. (I). Success criteria and epidemiology. *Eur J Oral Sci.*, 106:527-551.
  89. Misch CE, Hoar JE, Beck G et al. 1993. A bone quality-based implant system: a preliminary report of stage I and stage II. *Implant Dent.*, 15(suppl):554-561.
  90. Misch CE, Dietsch-Misch F, Hoar J et al. 1999. A bone quality-based implant system (BioHorizons maestro dental implants): a prospective study of the first year of prosthetic loading. *J Oral Implant*, 25:185-197.
  91. Kwan N, Yang S, Guillaume D, et al. 2004. Resistance to Crown Displacement on a Hexagonal Implant Abutment. *Implant Dentistry*, 13(2):112-119.
  92. Chiche GJ, Pinault A, Weaver C, et al. 1989. Adapting fixed prosthodontic principles to screw-retained restorations. *Int J Prosthodont.*, 2:317-322.
  93. Anderson B, Odman P, Lindvall AM. 1995. Single-tooth restorations supported by osseointegrated implants: results and experiences from a prospective study after 2 to 3 years. *Int J Oral Maxillofac Implants*, 10:702-711.
  94. Rosenthiel SF, Land MF, Crispin BJ. 1998. Dental luting agents: a review of the current literature. *J Prosthet Dent.*, 80:280-301.
  95. Kent D, Koka S, Froeschle M. 1997. Retention of cemented implant-supported restorations. *J Prosthet Dent.*, 6:193-196.
  96. Covey DA, Kent D, Germaine H, KoKa S. 2000. Effects of abutment size and luting cement type on the uniaxial retention force of implant-supported crowns. *J Prosthet Dent.*, 83:344-348.
  97. Yukna RA. 1993. Optimizing clinical success with implants: maintenance and care. *Compend Suppl.*, (15):554-561.
  98. Chakrapani S, Goutham M, Krishnamohan T. 2015. Periotest values: Its reproducibility, accuracy, and variability with hormonal influence. *Contemporary Clinical Dentistry*, 6(1):12-15.
  99. Oh JS, Kim SG, Lim SC, et al. 2009. A comparative study of two noninvasive techniques to evaluate implant stability: Periotest and osstell mentor. *Oral Surg Oral Med Oral Pathol Oral Radiol Endod.*, 107:513-518.
  100. Zix J, Hug S, Kessler-Liechti G, et al. 2008. Measurement of dental implant stability by resonance frequency analysis and damping capacity assessment: Comparison of both techniques in a clinical trial. *Int J Oral Maxillofac Implants*, 23:525-530.
  101. Lachmann S, Jäger B, Axmann D, et al. 2006. Resonance frequency analysis and damping capacity assessment. Part 1: An in vitro study on measurement reliability and a method of comparison in the determination of primary dental implant stability. *Clin Oral Implants Res.*, 17:75-79.
  102. Lachmann S, Laval JY, Jäger B, et al. 2006. Resonance frequency analysis and damping capacity assessment. Part 2: Peri-implant bone loss follow-up. An in vitro study with the Periotest and Osstell instruments. *Clin Oral Implants Res.*, 17:80-84.

\*\*\*\*\*